

AIAA 97-2745

INFLUENCE OF NOZZLE GEOMETRY ON THE PERFORMANCE OF A PULSE DETONATION WAVE ENGINE

W. S. Stuessy* and D. R. Wilson[§]
Aerodynamics Research Center
The University of Texas at Arlington
Arlington, Texas 76019

Abstract

Test results from an experimental investigation of the effect of nozzle geometry on the performance of a pulse detonation wave engine (PDE) are presented. Two detonation chamber geometries, cylindrical and annular, were tested. For each configuration, tests were conducted both with and without conical exhaust nozzles. The expansion angles of the nozzles were 9.52 and 14.24 deg. Data were obtained for stoichiometric mixtures of propane and oxygen, at a frequency of 20.4 to 28.5 Hz. Maximum performance was achieved with the annular configuration with the 14.24 degree nozzle.

Introduction

Air breathing engines based on the PDE cycle offer the promise of improved cycle efficiency and specific thrust, reduced specific fuel consumption and a wide operational range¹⁻³, whereas improvements in specific impulse have been demonstrated for pulse detonation rockets⁴. Moreover, significant weight and cost reductions are possible for both applications due to the reduced need for high-pressure turbomachinery. The chamber pressures required for achieving high thrust levels are generated by the detonation process. Furthermore, since PDEs can operate at very high energy densities, simple and compact combustor designs can be developed.

An excellent review of early historical developments of the PDE concept is given by Idleman, Grossmann and Lottati¹, whereas more recent developments are summarized in Refs. 5-13. Several groups, including UTA, have reported operational laboratory PDE's in the open

*Faculty Research Associate, Senior Member

[§]Professor of Aerospace Engineering, Associate Fellow
Copyright © 1997 by the American Institute of Aeronautics and Astronautics, Inc. All rights reserved

literature with frequencies on the order of 20 Hz. In order to produce an efficient PDE, however, frequencies between 50-100 Hz are needed. In general, the major problems hampering PDE development are the lack of efficient fuel/oxidizer injection systems, development of reliable energetic ignition systems, the necessity of purging residual combustion products between cycles, the need for accurate thrust measurements for repetitive cycle operation, and the actual attainment of sustained CJ detonation waves in a chamber of reasonable length.

Theory of Operation

A detonation chamber pressure profile based on the classical Zeldovich-von Neumann-Doring (ZND) model is shown schematically in Fig. 1 (adapted from Ref. 2). The shock front is moving from left to right into an unburned fuel-air mixture. The high pressure region of unburned gas behind the shock is known as the von Neumann spike. Following a short ignition delay, typically on the order of 1 μ s, chemical reactions are initiated and the energy release causes a decrease in pressure and an increase in temperature to levels predicted from Chapman-Jouguet theory. An unsteady expansion is generated at the closed end of the chamber to satisfy the zero velocity boundary condition which reduces p_2 to the end-wall pressure p_3 . It is this pressure acting on the end-wall, together with the pressure forces generated in the subsequent downstream nozzle expansion, that produce the thrust of a PDE.

Our research has shown that rapid development of a Chapman-Jouguet (CJ) detonation wave is crucial for maximizing thrust¹⁰. In most instances, the ignition process is not energetic enough to directly initiate a CJ wave, and a deflagration or weak detonation is initiated which transitions to a CJ detonation some distance downstream of the ignition source. The length of the deflagration-to-detonation transition (DDT) can adversely affect the length of the engine. Generally, techniques to

reduce the DDT length make use of various turbulence generators such as a Shchelkin spiral, wire ring, or orifice plate^{9,10}. The effect of a Shchelkin spiral on end-wall pressure is shown in Fig. 2 for a detonation chamber containing a stoichiometric mixture of hydrogen and oxygen at an initial pressure of 1 atm. A gradual rise in pressure is initially observed, followed by an abrupt transition to a level of about 120 psia at $t \approx 14.5$ ms. This pressure rise correlates with the observed transition to a fully-developed CJ detonation. In similar tests conducted without the spiral, the end-wall pressure never exceeded 70 psia. The subsequent sharp rise at 14.75 ms is due to the return of the reflected detonation wave from the downstream diaphragm, and would not be present in an actual PDE. Similar results were observed for propane/oxygen mixtures that naturally transitioned to CJ detonation waves, except that end-wall pressure levels of 220 psia were measured for this mixture. Both of these end-wall pressure levels agree well with theoretical calculations.

Previous studies have shown that detonation waves are actually rhombic cellular structures^{14,15}, rather than simple one-dimensional waves as assumed in the Chapman-Jouguet or ZND models. Lefebvre and Oran¹⁵ suggested that the detonation structure can be viewed as a series of interactions between incident shock fronts, Mach stems, transverse shock waves and the walls of the chamber. These studies show that transverse waves play an important role in the propagation and sustenance of detonations. An example of a computed detonation cell, with the transverse waves highlighted, is shown in Fig. 3. In this figure, the horizontal axis marks the timesteps at a given location while the shading indicates pressure levels; the darker the shade the higher the pressure. Lefebvre and Oran found that the shock intersections (or so-called "triple points") associated with the transverse waves are regions of high density and vorticity. They are also regions of large heat release and are shown as dark bands in enlarged sketches a through c in Fig. 3. Since detonation cells move with the CJ wave, the triple points move transversely in concert with the movement of the transverse waves. This means that the regions of large heat release also propagate transversely and these are thought to contribute to mixing enhancement via a type of Rayleigh-Taylor instability¹⁵. It has been suggested that turbulence generators, which

accelerate the turbulent flame front and cause DDT, trigger the formation of transverse waves¹⁶.

A Pulse Detonation Engine operates by filling a chamber with a fuel and oxidizer combination, then detonating the mixture with a suitable ignition source. The detonation wave and combustion products are allowed to exit the chamber to provide thrust. After the detonation wave exits the chamber the pressure equilibrates to the local ambient pressure through a series of expansion and compression waves that reverberate through the chamber. The chamber can then be refilled with fuel and oxidizer and the cycle repeated. The fuel and oxidizer are injected at low pressure and then detonated to obtain the high pressures required for thrust production.

CFD simulations of the PDE cycle show that the pressure of the residual combustion products quickly drop to the ambient pressure but the temperature remains very hot for an extended period of time (Fig. 4). The temperature is hot enough to cause auto ignition of the fuel and oxidizer upon injection. This auto ignition is of a deflagration nature, and prevents the attainment of successive detonation waves. Auto ignition can be prevented by injection of purge air between cycles, but this must be done with care to prevent excessive penalties in specific impulse. The maximum frequency attainable by a PDE is a complex function of the interplay between the fueling, ignition, detonation wave formation and propagation, blowdown and purge air injection processes.

Test Facility

The PDE test facility was originally designed to study detonation wave phenomena, and is described in detail in Ref. 10. The test facility consists of a test chamber, fuel and oxidizer system, purge air system, high-energy arc ignition system, instrumentation, and high-speed data acquisition/control system. It was modified to investigate phenomena associated with the repetitive operation of a PDE, and initial test results were presented in Refs. 11 and 13.

Test Chamber

A schematic of the detonation chamber is shown in Fig. 5. The detonation chamber has a fixed internal diameter of 7.62 cm (3 inch) and three sections of different length. The first 7.62 cm (3 inch) section contains an arc igniter plug at its center. The ignition section is followed by a 30.48

cm (12 inch) and a 15.24 cm (6 inch) section, for a total length of 53.34 cm (21 inch). The last section can be replaced by an equivalent length diverging nozzle section with either a 9.52 or 14.24 deg conical expansion angle. Each section of the chamber has provisions for mounting pressure transducers, thermocouples, and Gardon-type heat flux gauges at 7.62 cm (3 inch) intervals. A 2.54 cm (1 inch) diameter center body can be installed throughout the length of the chamber to create an annular configuration. For the nozzle tests, the center body was truncated with a conical spike of approximately the same length as the conical nozzle section.

Injection System

The injection system was designed for use with either hydrogen, propane, or methane as fuels and oxygen or air as oxidizers. The fuel and oxidizer are injected into the chamber through rotary valves mounted on an endplate which seals one end of the chamber. They are injected perpendicular to the axis of the chamber in such a way as to impinge upon each other during the injection process to promote mixing. The fuel and oxidizer flow rates are controlled by setting the valve supply pressure according to regulator flow rate charts. Purge air is also injected at the proper time between cycles to provide a buffer between the residual combustion products of one cycle and the injected reactants of the next cycle. The purge air is injected using a third rotary valve. The rotary valves are driven by a frequency-controlled variable-speed electric motor. A magnetic pickup is located nearby to sense the closure of the valves and initiate the ignition process. A second air line is used for purging of the explosive gases in the advent of a misfire. The opposite end of the chamber is open to atmosphere for exhaust of the detonation wave and combustion products.

Ignition System

The ignition system consists of a high-voltage, high-current arc plug driven by a capacitor bank discharge. The arc plug is mounted in a 7.62 cm (3 inch) tube section which can be placed at either end of the detonation chamber. Breakdown of the gap between the electrodes is initiated by a high frequency arc welding source. Once the gas is sufficiently ionized, the arc is sustained by the discharging a capacitor bank connected to the electrodes.

An electrical schematic of the ignition system is shown in Fig. 6. The discharge capacitor bank consists of two 11000 microfarad 75 V DC capacitors connected in series and charged to about 135 V DC. A second charge capacitor bank, identical to the discharge capacitor bank, is used to recharge the discharge capacitor bank between cycles and is kept at 135 V DC by a 1.2 kVA variable transformer and a rectifying diode bridge. The two capacitor banks are isolated by means of a thyristor. The thyristor switches on just long enough to recharge the discharge capacitor bank and then turns off. If the two capacitor banks are not isolated during the arc discharge both capacitor banks will discharge simultaneously, and the variable transformer will begin driving the arc in a welding mode. This draws large amounts of current which can lead to rapid heating and possible destruction of certain components. Minimizing the discharge time results in more energy transferred to the gas and less to the structure of the arc plug for the same energy discharge from the capacitor. The charge capacitor bank is used to even out the current flow through the variable transformer and allow the discharge capacitor bank to be recharged more quickly. The outputs of the discharge capacitor bank were connected together with a diode to eliminate ringing of the discharge current. This eliminates reverse voltage on the capacitor bank and reduces the maximum voltage differential seen by the thyristor. The thyristor is controlled by a timer circuit (Fig. 7) that also initiates the high frequency welding unit, sets the proper time delay for recharging the discharge capacitor bank, and provides the signal to the thyristor.

The energy from the discharge capacitor bank is discharged through an arc plug consisting of two tungsten electrodes encased in ceramic and mounted in a threaded steel housing. The ends of the electrodes are flush with the surface of the ceramic. The threaded housing assembly is then installed into the ignition tube section so that the electrodes are nearly flush with the inner wall of the detonation chamber.

Instrumentation

The primary instrumentation used in the current test program consisted of six PCB model 111A24 piezoresistive pressure transducers which were individually water cooled for continuous multi-cycle operation. The PCB transducers have a full scale range of 6.89 MPa (1000 psi), rise time of 2

μs , and a time constant of 100 s. The initial reference for the PCB transducers is local atmospheric pressure, which is measured by a MKS model 127A Baratron pressure transducer. It has a maximum range of 1333 kPa (10000 Torr). Local heat flux measurements were made with four Gardon-type heat flux gages. These gages have a full scale range of $45,425 \text{ kw/m}^2$ ($4000 \text{ BTU/ft}^2 \text{ sec}$) and a response time of 50 msec. The pressure transducers were mounted at 7.62 cm (3 inch) intervals, with the first transducer being located 7.62 cm (3 inch) downstream of the igniter. The four heat flux gages were installed opposite of the four pressure transducers closest to the open end of the chamber.

The pressure and heat flux sensors were connected to a 48 channel DSP Technology data acquisition system. Each channel has a dedicated amplifier and 12 bit analog to digital converter. All 48 channels can be sampled simultaneously at a rate of 100 kHz. The DSP system has 512 Kilobytes of memory available for distribution among the channels being utilized. Eight channels are also available with the capability of 1 MHz sampling rate, with separate 12-bit analog to digital converters for each channel. Two Megasamples of memory are available for these eight channels. The data acquisition system is placed adjacent to the test facility and connected to a PC located in the adjoining control room via an IEEE-488 interface bus. Test data are then stored on a harddrive for later analysis.

Data Analysis

Voltage readings from the pressure transducers were converted into pressure readings using calibration curves provided by the manufacturer and plotted against time. The time interval between the observed rise in pressure from adjacent transducers was used to calculate the propagation speed of the detonation wave. The manufacturer's calibration curves were also used for the heat flux gages.

A conventional uncertainty analysis¹⁷ resulted in the following error estimates for the principle test variables:

Pressure:	$\pm 5.4\%$
Heat flux:	$\pm 3.0\%$
Wave speed:	$\pm 10.0\%$ (100 kHz)
	$\pm 1.4\%$ (1 MHz)

The 100 kHz sampling rate was used for the pressure measurements used to calculate wave speeds for the data reported in this paper. However, previous tests in which the data were scanned at 1 MHz indicate that the wave speeds obtained from the 100 kHz sampling rate are more accurate than the error analysis would suggest, and in fact agree quite closely with results from the 1 MHz sampling rate. An error analysis was not performed on the mixture ratio, which is the other principal test variable. We have yet to develop an accurate method for measuring the pulsating flow rates of the fuel and oxidizer. The procedure used for the current test program involved setting flow rates to give near-stoichiometric mixture ratios using published calibration charts for the pressure regulators. The flow rates were then fine-tuned to give optimum performance. Thus, the mixture ratios can only be stated as near-stoichiometric with any degree of confidence.

Test Matrix

The test matrix consisted of the following variables:

Chamber geometry:	Cylindrical, Annular
Nozzle divergence:	0, 9.52, 14.24 deg
Fuels:	Propane
Oxidizer:	Oxygen
Mixture ratio:	Stoichiometric
Frequency:	20 - 28 Hz

Results

Pressure and Velocity Data

Pressure vs. time plots showing propagation of the detonation wave through the chamber are shown in Fig. 8 for the basic cylindrical configuration. The frequency for this test was 20.6 Hz. The shape of the pressure plots are indicative of a weak detonation wave in that a gradual rise in pressure is observed as the detonation wave approaches the various transducer stations. Fully developed CJ detonation waves do not exhibit this precompression phenomena but instead are characterized by a sharp rise in pressure. Furthermore, calculation of the average wave propagation speed yields a value of about 890 m/s, compared to the theoretical CJ wave speed of 2360 m/s for a stoichiometric mixture of

propane and oxygen. Also the peak pressures are much lower than theoretical CJ pressures.

A similar plot for the annular configuration with a 14.24 deg exhaust nozzle is shown in Fig. 9 for comparison. The frequency for this run was 24.8 Hz. These pressure traces show less pre-compression and a slightly higher peak pressure. The average velocity for this case is 1040 m/s, which is higher than the average velocity for the cylindrical configuration, but still considerably below the theoretical CJ velocity.

A plot showing pressure variation with time from the transducer located near the exit of the chamber is shown in Fig. 10. This particular plot was from the annular configuration with the 14.24 deg exhaust nozzle. Measurement of the time between peak pressures yields a frequency of 25 Hz. Some irregularity in repetition of the peak pressure level is observed, and is caused by the electronics in the control system. The particular procedure used to initiate the ignition sequence has a minimum resolution of 8-9 msec, thus the ignition process does not always occur at the precise time required for optimum performance. A new design has been developed that should reduce the timing resolution to 0.1 msec, and will soon be installed.

An expanded plot of Fig. 10 showing pressure vs. time for one complete blowdown cycle is shown in Fig. 11, and a similar plot for the cylindrical configuration is shown in Fig. 12. The traces are quite similar, and the addition of the nozzle does not appear to significantly affect the blowdown process. The chamber pressure equilibrates to atmospheric pressure in about 18-20 msec in both cases.

The pressure vs. time plots were converted to velocity vs. distance plots, and the results are presented in Figs. 13 and 14. These results clearly show a higher wave propagation speed for the annular configurations, which is consistent with previous results obtained with hydrogen^{10,13}. The inclusion of the nozzle also appears to improve performance in that, with the exception of the cylindrical configuration with the 14.24 deg nozzle, the wave propagation speed does not fall off near the exit as it does for the configurations without the nozzle.

Comparison with Hydrogen Data

A velocity vs. distance plot for a similar test conducted with stoichiometric hydrogen/oxygen

mixtures is shown in Fig. 15 (from Ref. 13). The engine frequency for this data was 11 Hz, however, the effect of frequency in this range is relatively minor. Several differences in the velocity plots are immediately obvious. First, the initial velocities were near sonic for the hydrogen cases, whereas, initial velocities for propane are supersonic, with Mach numbers on the order of 1.9 to 4.3. However, the velocities do not increase for the propane runs, whereas a definite increase in velocity with distance from the igniter is seen with hydrogen. A comparison of pressure traces shows that in general, higher pressures were obtained with hydrogen.

Heat Flux Results

Typical results from the heat flux measurements are shown in Figs. 16 and 17. The data are from the annular configuration with the 14.24 deg nozzle. The data in Fig. 16 is from a gage located in the detonation chamber, whereas the data in Fig. 17 are from a gage located near the nozzle exit. The heat flux has a cyclical variation with a frequency that matches the engine operating frequency. The heat flux gages have much lower response characteristics than the pressure transducers, thus they do not follow the pressure variations observed during the blowdown portion of each cycle. The heat flux in the nozzle is about 70 percent of that in the detonation chamber. Heat flux measurements from the other configurations were similar, and no significant differences were observed for the different configurations.

Conclusions and Recommendations

Results from an experimental investigation of the effect of nozzle geometry on the performance of a PDE were reported for a series of tests using near stoichiometric propane/oxygen mixtures. In general, the inclusion of a conical exhaust nozzle improved performance in that higher wave propagation speeds were maintained in the downstream part of the detonation chamber. Direct thrust measurements were not made, but the higher wave speeds should lead to an increase in thrust over that attainable from configurations without an exhaust nozzle. The nozzle did not significantly affect the blowdown process. Essentially identical equilibration times were achieved with or without the nozzle. Measured heat transfer rates in the nozzle were about 70 percent of the level measured in the detonation chamber. Maximum performance, as

characterized by detonation wave propagation speed, was achieved for the annular configuration with the 14.24 deg nozzle.

Future experiments will include a repetition of the tests reported in this paper with hydrogen fuel. Furthermore, a new side-wall fuel injection system has been installed that together with a new high-frequency ignition system, should allow further increases in engine operating frequency. The design goal is a frequency of 100 Hz, with sustained CJ detonation waves. This will, in all probability, require the inclusion of turbulence generators such as a Shchelkin spiral.

Acknowledgements

This material is based in part upon work supported by the Texas Advanced Technology Program under Grant No. 003656-031. The CFD simulations shown in Fig. 4 were provided by Mr. B.D. Couch of Lockheed Martin Tactical Aircraft Systems.

References

- ¹Eidelman, S., Grossmann, W. and Lottati, I., "Review of Propulsion Applications and Numerical Simulations of the Pulsed Detonation Engine Concept," *Journal of Propulsion*, Vol. 7, No. 6, Nov.-Dec., 1991, pp. 857-865.
- ²Bussing, T. and Pappas, G. "An Introduction to Pulse Detonation Engines," AIAA Paper 94-0263, 1994.
- ³Eidelman, S., Yang, Y. and Lottati, I., "Pulsed Detonation Engine: Key Issues," AIAA Paper 95-2754, 1995.
- ⁴Black, L.H. and Varsi, G., "Detonation Propulsion for High Pressure Environments," *AIAA Journal*, Vol. 12, No. 8, Aug. 1974, pp. 1123-1130.
- ⁵Cambier, J.J. and Adelman, H.G., "Preliminary Numerical Simulations of a Pulse Detonation Wave Engine," AIAA Paper 88-2960, 1988.
- ⁶Lynch, E.D., Edelman, R. and Palaniswamy, S., "Computational Fluid Dynamic Analysis of the Pulse Detonation Engine Concept," AIAA Paper 94-0264, 1994.
- ⁷Eidelman, S., Grossmann, W., Gunners, N.-E. and Lottati, I., "Progress in Pulsed Detonation Engine Development," AIAA Paper 94-2721, 1994.
- ⁸Sterling, J., Ghorbanian, K., Humphrey, J., Sobota, T. and Pratt, D., "Numerical Investigations of Pulse Detonation Wave Engines," AIAA Paper 95-2479, 1995.
- ⁹Hinke, J.B., Bussing, T.R.A. and Kaye, L., "Shock Tube Experiments for the Development of a Hydrogen-Fueled Pulse Detonation Engine," AIAA Paper 95-2578, 1995.
- ¹⁰Stanley, S., Burge, K. and Wilson, D., "Experimental Investigation of Pulse Detonation Wave Phenomenon as Related to Propulsion Application," AIAA 95-2580, 1995.
- ¹¹Stuessy, W.S. and Wilson, D.R., "Experimental Investigation of a Multi-Cycle Pulsed Detonation Wave Engine," AIAA Paper 96-0346, 1996.
- ¹²Lynch, E.D. and Edelman, R.B., "Analysis of the Pulse Detonation Wave Engine," in "Developments in *High-Speed Vehicle Propulsion Systems*," ed. by S.N.B. Murthy and E.T. Curran, AIAA, Reston, VA, 1996.
- ¹³Stuessy, W.S. and Wilson, D.R., "Experimental Investigation of an Annular Pulse Detonation Wave Engine," AIAA Paper 97-0808, AIAA 35th Aerospace Sciences Meeting, Reno, Nevada, January 6-9, 1997.
- ¹⁴Lefebvre, M.H. and Oran, E.S., "Analysis of the Shock Structures in a Regular Detonation," *Shock Waves*, 4(5):277-283, 1995.
- ¹⁵Bauwens, L. and Williams, D.N., "Computation and Visualization of Detailed Detonation Structures," AIAA Paper 96-0343, 1996.
- ¹⁶Kratzel, T., Pantow, E. and Eichert, H., "Modeling of Hydrogen Combustion: Turbulent Flame Acceleration and Detonation," *International Journal of Hydrogen Energy*, 21(5):407-414, 1996.
- ¹⁷Kline, S.J. and McClintock, F.A., "Describing Uncertainties in Single-Sample Experiments," *Mechanical Engineering*, Vol. 75, 1953.

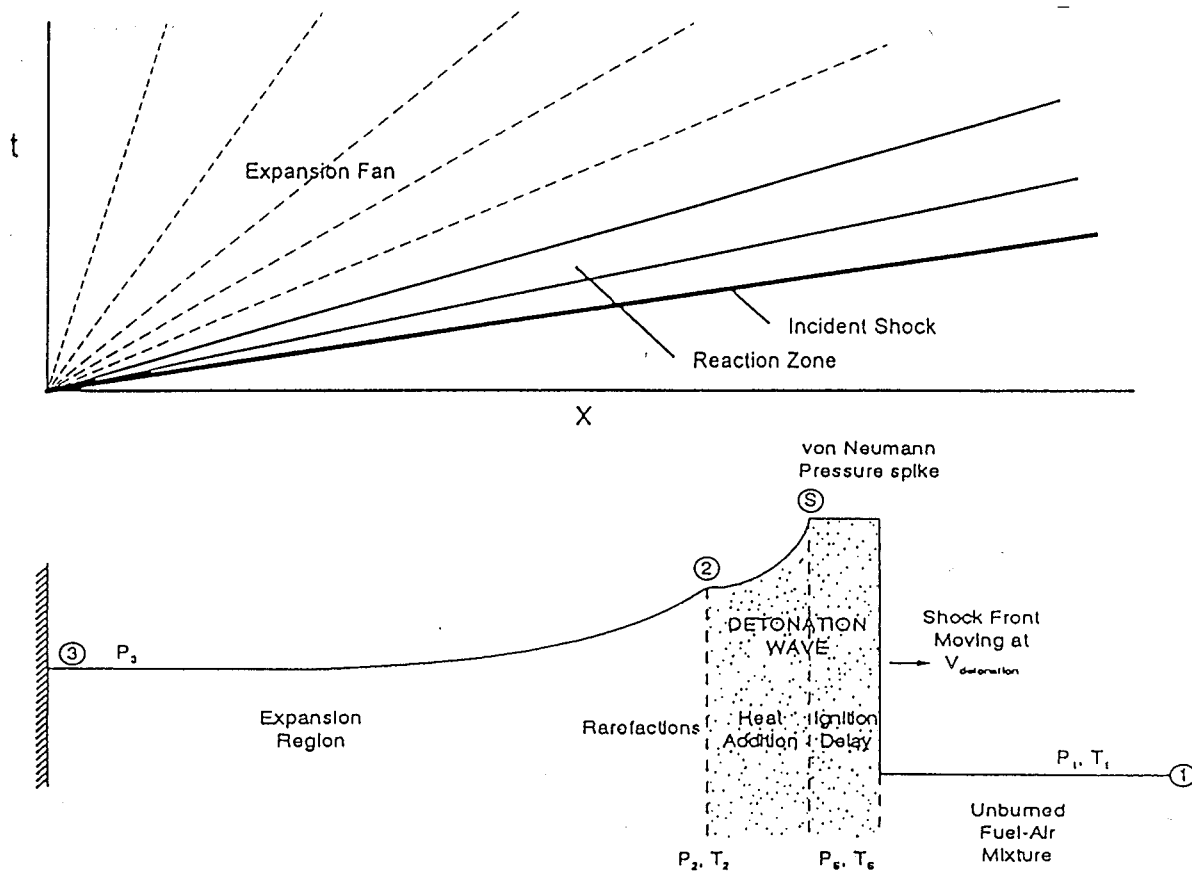


Fig. 1 ZND detonation wave model (adapted from Ref. 2)

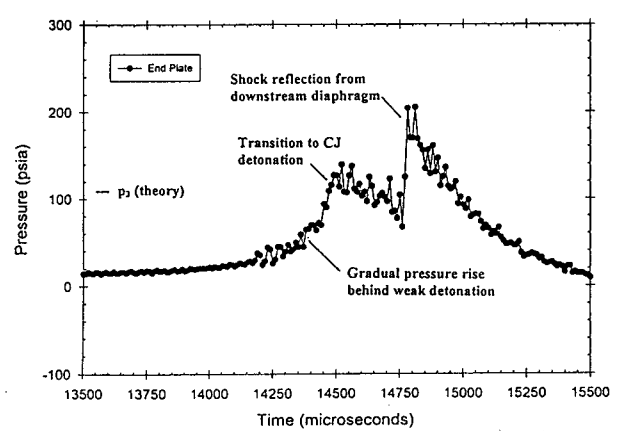


Fig. 2 End-wall pressure, stoichiometric mixture of H_2/O_2 at 1 atm

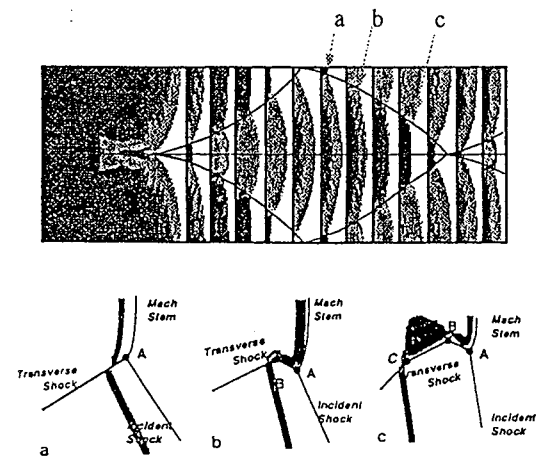


Fig. 3 A detonation cell showing complex wave formation (from Ref. 14)

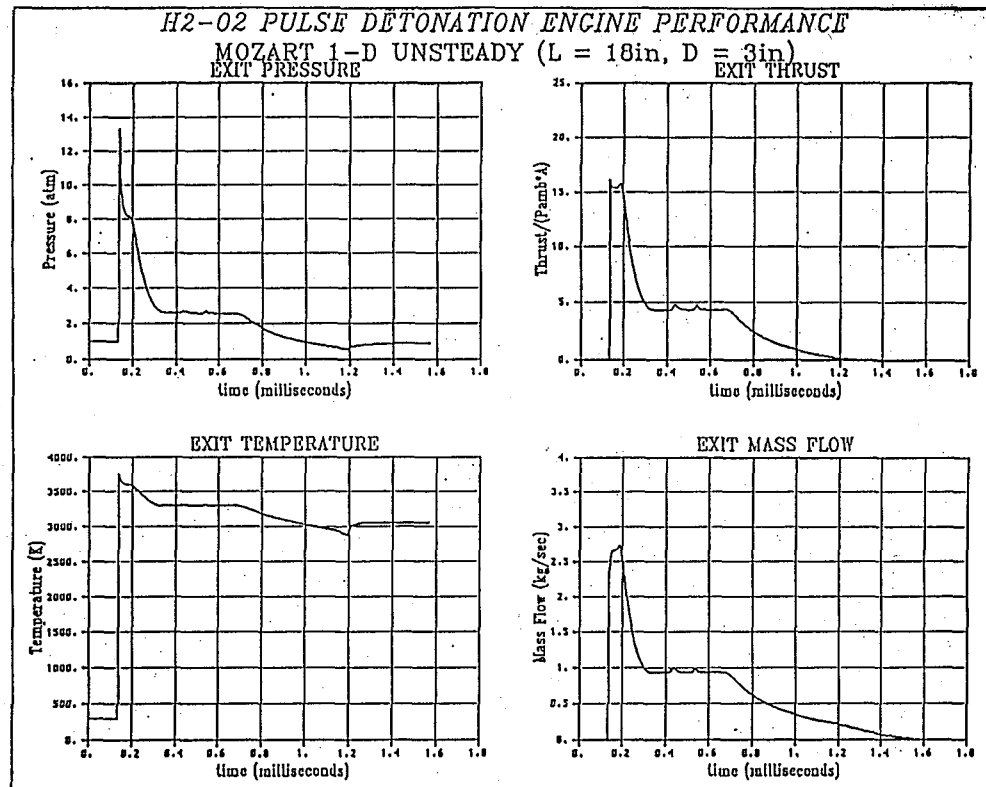


Fig. 4 CFD Simulation of the PDE cycle
 (Courtesy of B.D. Couch, Lockheed Martin Tactical Aircraft Systems)

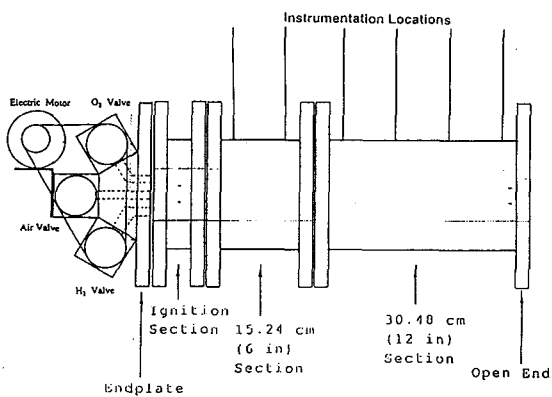


Fig. 5. Detonation chamber schematic

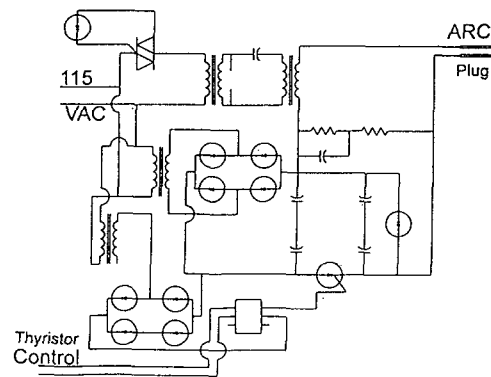


Fig. 6 Ignition system schematic

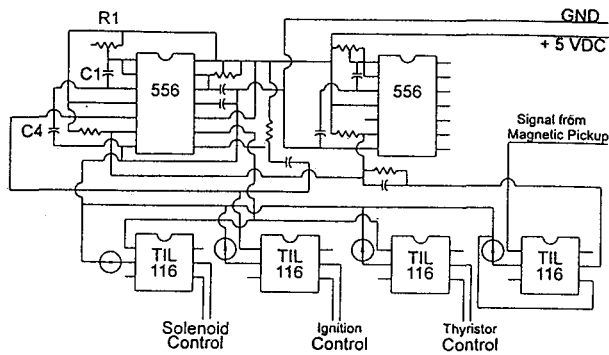


Fig. 7 Electronic control circuit

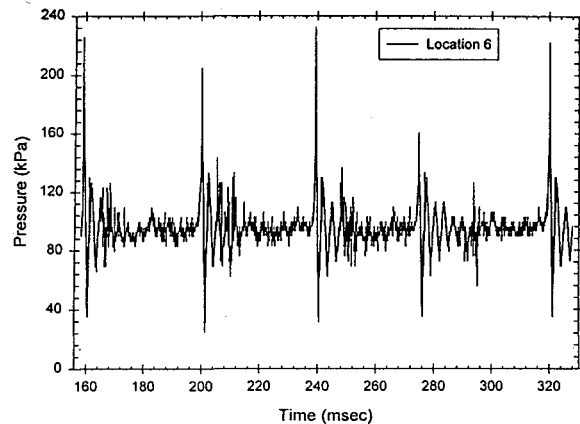


Fig. 10 Nozzle exit pressure vs. time. annular configuration at 25 Hz

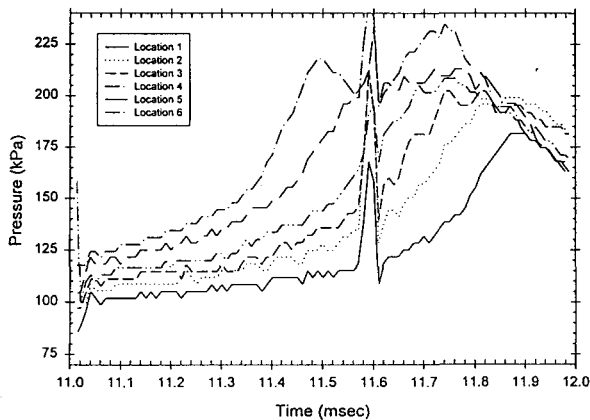


Fig. 8 Detonation chamber pressure vs. time, basic cylindrical configuration

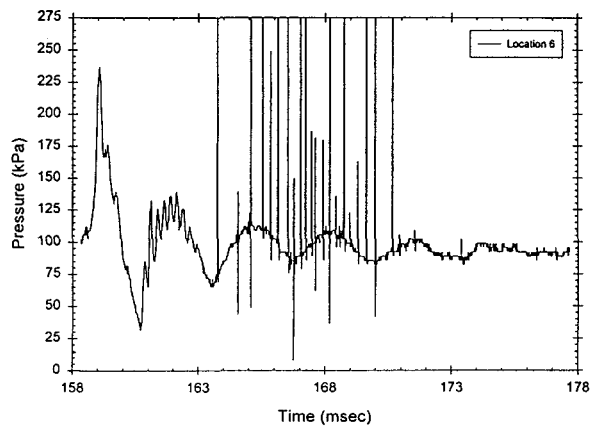


Fig. 11 Nozzle exit pressure vs. time for one cycle, annular configuration with 14.24 deg nozzle

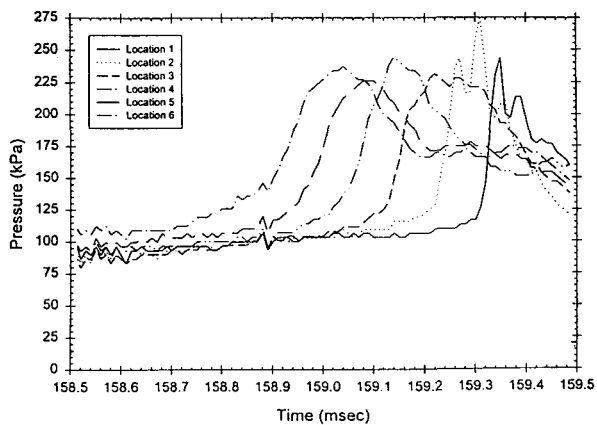


Fig. 9 Detonation chamber pressure vs. time, annular configuration with 14.24 deg nozzle

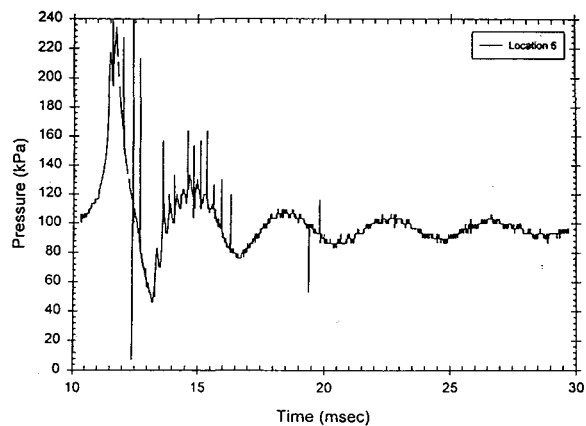


Fig. 12 Nozzle exit pressure vs. time for one cycle, cylindrical configuration

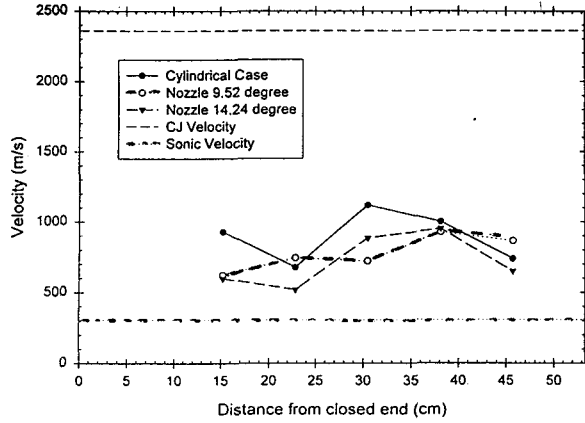


Fig. 13 Velocity vs. distance, cylindrical configuration

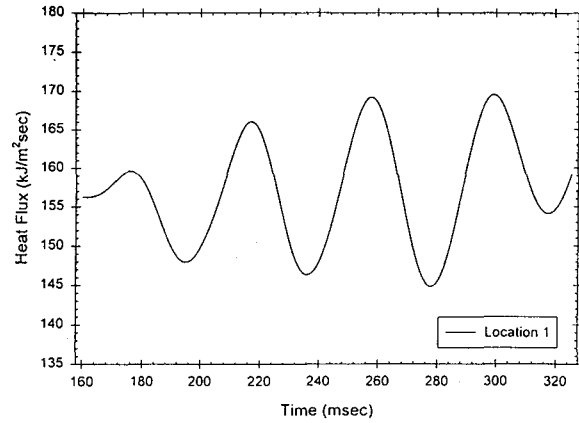


Fig. 16 Detonation chamber heat flux, annular configuration with 14.24 deg nozzle

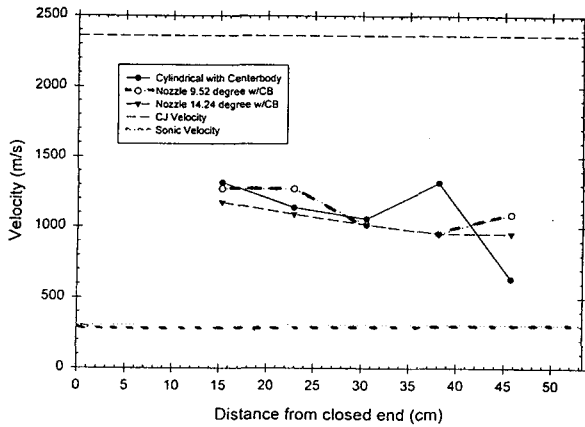


Fig. 14 Velocity vs. distance, annular configuration

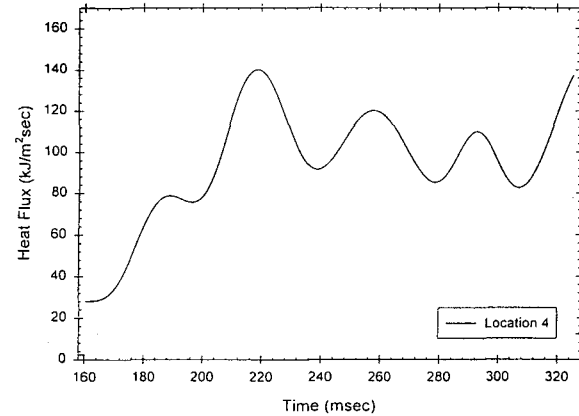


Fig. 17 Nozzle heat flux, annular configuration with 14.24 deg nozzle

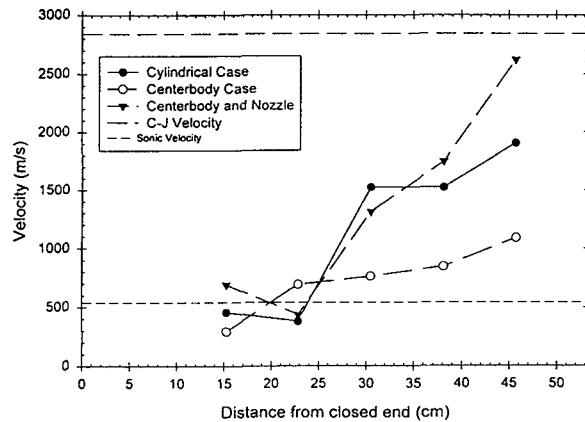


Fig. 15 Velocity vs. distance plot, hydrogen/oxygen (from Ref. 13)